# PARTICLE IMAGE VELOCIMETRY USING OPTICAL FLOW FOR IMAGE ANALYSIS

Georges M. Quénot, Jaroslaw Pakleza  Tomasz A. Kowalewski

**Keywords:** *Particle Image Velocimetry, Optical flow*

**Abstract**

*The aim of our investigation was to explore a new method of analysing flow images, based on the Optical Flow Technique. Conventionally, this technique was developed for detecting motion of large objects in a real world scene. Applied to the flow images, it appears to be an interesting alternative offering high evaluation accuracy without most of the typical limitations characteristic of FFT based PIV. Besides evaluation of tracer images, the new method was also tested with smoke images obtained from experiments both in a fluidised bed and in a wind tunnel. It was also successfully tested on an image sequence of a vapor bubble growing on a thin heated wire. The accuracy of the velocity measurements using the new implementation was investigated using synthetic particle image sequences generated with the help of a 2D numerical simulation.*

## 1 Introduction

The aim of this investigation is to explore the possibility of using an optical flow technique in measuring fluid flow velocity. Classical flow visualization is based on direct observation of tracer particles. Analysis of subsequent images searching for local displacements allows quantitative measurement of two-dimensional flow fields. The optical flow method offers a new approach for analysing flow images. It largely improves spatial accuracy and minimizes the number of spurious vectors. Application of this method may help in quantitative analyses of several challenging problems of fluid mechanics, as well as in full plane validation of their numerical counterparts. Moreover, the optical flow method is able to track not only tracer particle but also various textured items including smoke and bubbles.

## 2 Particle Image Velocimetry

Recently, the experimental fluid mechanics technique of Particle Image Velocimetry (PIV) has proven to be a valuable method for quantitative, two-dimensional flow structure evaluation. It enables the measurement of the instantaneous in-plane velocity vector field within a planar section of the flow field. The classical PIV technique uses multiple-exposure images and optical autospectrum or autocorrelation analysis [2].

Conventionally, PIV images are recorded on photographic film, and the flow field is obtained via the computation of the spatial correlation into small search regions. The point-by-point search analysis is repeated until the entire negative is analyzed. Processing large numbers of such images becomes a very laborious task. Therefore, an alternative approach - referred as Digital Particle Image Velocimetry (DPIV) - was introduced [17], [16]. Images are recorded directly with a CCD camera and frame-grabber, and can be studied without the unnecessary de-

*Received December 22, 1997. Accepted February 28, 1998.*

*Contact author: Georges M. Quénot, Jaroslaw Pakleza[1], Tomasz A. Kowalewski[2]*

[1]LIMSI-CNRS, BP133, F-91403 Orsay Cedex, France
[2]Polish Academy of Sciences, IPPT PAN, PL 00-049 Warszawa

lay and overhead associated with the scanning of photographs. The application of DPIV allows for a simple realization of the cross-correlation technique for pairs of two separate images. It removes the ambiguity of the sign of the displacement and improves signal dynamics. Despite recent progress in the DPIV development, further improvement of the accuracy and minimization of the computational time still remains a current research goal [4], [13].

One of the main drawbacks of classical DPIV is its inability to accurately resolve flow regions characterized by large velocity gradients. This is due to the strong deformation of the particle image pattern within a DPIV search window. Hence, several alternative evaluation methods have been proposed to remove the above limitation [3], [15], [6]. With this in mind, it appeared to us that an *optical flow* method may be an interesting alternative, offering high evaluation accuracy without most of the typical DPIV limitations. Conventionally, this technique was developed for detecting motion of large objects in a real world scene. The idea of this evaluation technique is in some sense similar to the Image Correlation Velocimetry proposed by Tokumaru and Dimotakis [15].

## 3 Optical Flow Computation

Optical flow computation consists in extracting a dense velocity field from an image sequence assuming that the intensity (or colour) is conserved during the displacement. Many techniques have been developed for the computation of optical flow. In a survey and a comparative performance study, Barron et al. [1] classify them into four categories: differential, correlation based, energy based, and phase based. Not all of these are well suited for the DPIV problem. Many require long image sequences that are not easily obtainable experimentally and/or do not perform very well on the particle image texture (especially multi-resolution methods).

The technique that was chosen for the DPIV application was introduced by Quénot [8] as the Orthogonal Dynamic Programming (ODP) algorithm for optical flow detection from a pair of images. It has been extended to be able to operate on longer sequences of images and to search for subpixel displacements [9]. The ODP based DPIV will be referred to as ODP-PIV. Compared with other optical flow approaches or to the classical correlation based DPIV, the ODP-PIV has the following advantages:

- It can be applied simultaneously to sequences of more than two images.
- It performs a global image match by enforcing continuity and regularity constraints on the flow field (this helps in ambiguous or low particle density regions).
- It provides dense velocity fields (neither holes nor border offsets).
- Local correlation is iteratively searched for in regions whose shape is modified by the flow, instead of being searched in fixed windows. This greatly improves the accuracy in regions with strong velocity gradients.
- It is able to operate on multiband (e.g. colour) images.

Only a short description of the ODP algorithm is given here. Details and extensions can be found in [8], [9] and [11]. Another extension of interest for DPIV is the possibility to generate a continuous sequence of intermediate images between a pair of images using the extracted velocity field [10]. This allows to visualize more clearly the flow structure and to check the correctness of the extracted flow field.

Dynamic Programming is a very robust technique for searching optimal alignments between various types of patterns because it is able to include order and continuity constraints during the search. However, it is applicable only for the search of monodimensional alignments (the reason is that no natural order can be found for a multidimensional set) and uneasy to use directly for image matching.

The originality of the Orthogonal Dynamic Programming (ODP) algorithm is that it transforms the search problem for two-dimensional alignments into a carefully selected sequence of search problems for monodimensional alignments. It is based on an iterative search for a velocity field that brings the second image over the first one while minimizing the $L_1$ or $L_2$ (Minkowski) distance between them.

Both images are sliced into parallel and overlapping strips (Figure 1). Corresponding strips are aligned (Figure 2) using dynamic programming exactly as 2D representations of speech signal are with the Dynamic Time Warping algorithm [12].

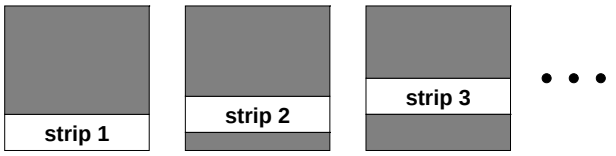


**Fig. 1.** Image slicing

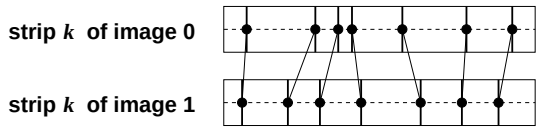


**Fig. 2.** Image slicing

An optimal segment to segment alignment is searched for as a continuous and increasing path inside the disparity matrix along which the sum of the local distance (segment to segment $L_1$ or $L_2$ distance) is minimum (Figure 3).

A dense velocity field is build (or updated) for the whole image by interpolation and smoothing using the relative velocity values obtained for the strips central lines. Two passes are performed using orthogonal slicing directions. This process is iterated in a pyramidal fashion by reducing the spacing and width of the strips to refine the accuracy of the matching result (Figure 4). The width of the search window around the diagonal of the disparity matrix

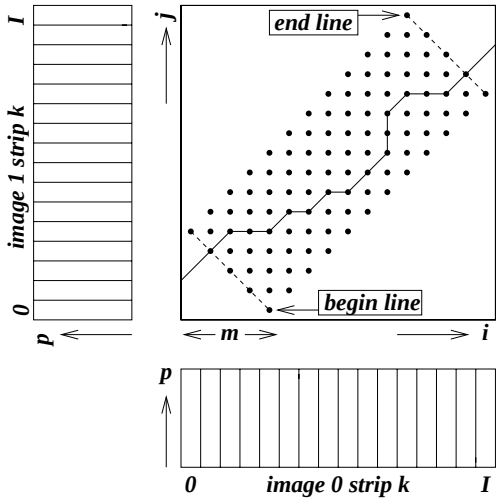


**Fig. 3.** Image slicing

is also reduced during the iterative process. At every new iteration, the alignment is searched in a new direction and/or at a new resolution on the original images rectified using the velocity field obtained from the previous iterations.

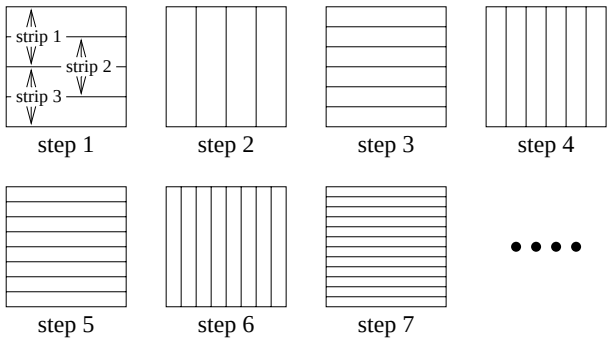


**Fig. 4.** Image slicing

## 4 Calibration on synthetic images

Several test sequences of four images were generated using a synthetic image representative of the random particle texture and a velocity field taken from a numerical solution obtained for two-dimensional flow around pair of cylinders [5]. They are available for comparative evaluations from the public LIMSI ftp server at: `ftp://ftp.limsi.fr/pub/quenot/opflow/-testdata/piv`. For each sequence, the images, numbered from 0 to 3, represent particle

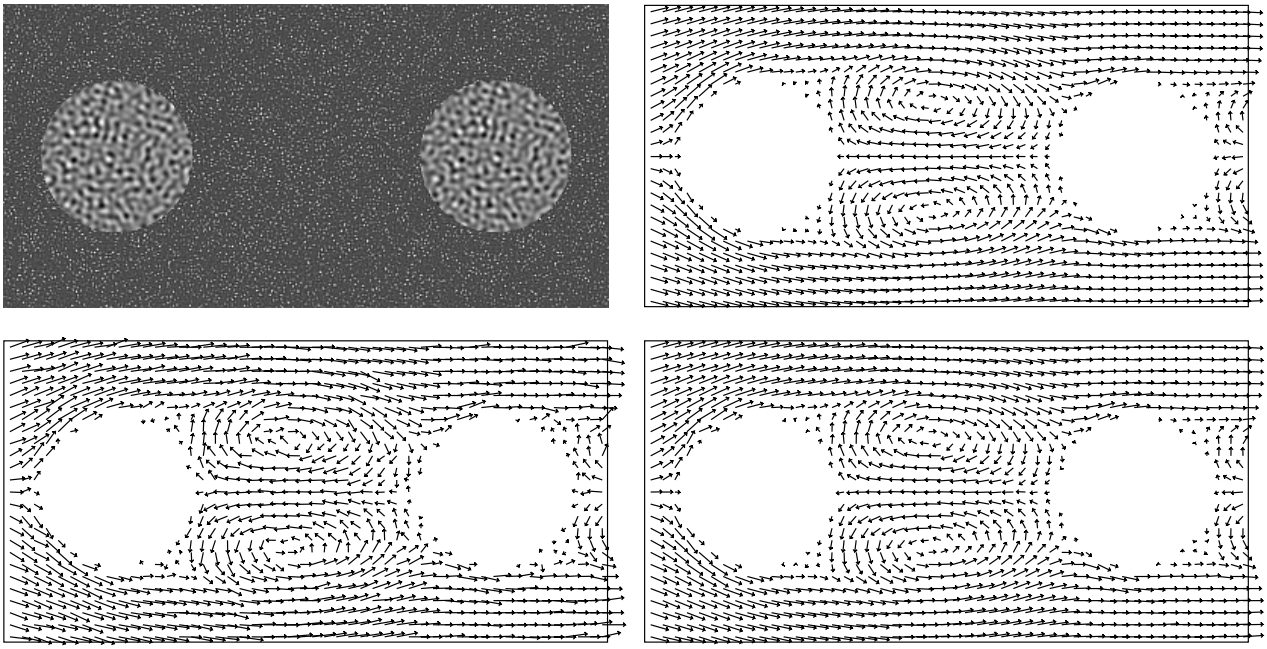

**Fig. 5.** Synthetic particle sequence (four 800 × 400 images). Top left: synthetic particle image; top right: original reference velocity field (subsampled 16 times horizontally and vertically), average velocity module is 7.58 pixel/frame; bottom left and right: recovered velocity fields from two images and four images under worst case conditions (20% of additive noise and 20% of particles added or removed). Velocity fields are displayed using a non linear scale.

textures calculated at four time steps: $-3/2$, $-1/2$, $1/2$ and $3/2$. The velocity field $v$ is defined (and searched for) in the "central" image of the sequence (which has the image index $3/2$). Images 0, 1, 2 and 3 are generated by applying the velocity fields $-3v/2$, $-v/2$, $+v/2$, and $+3v/2$ respectively to the central image. The central image is not a part of the sequence.

The sequence labelled "Perfect" is generated ideally from the velocity field and the texture image. The sequences labelled "Noise $N$%" are identical to the "Perfect" sequence except that the intensity of all four images is modulated by adding to each pixel randomly generated noise from the interval $[-255.N/100, 255.N/100]$ (with saturation in case of overflow or underflow). The sequences labelled "Add/rm $N$%" are identical to the "Perfect" sequence except that $N$% of the particles are randomly removed and $N$% of other particles are randomly added between the first and the last image. For the intermediate images, these particles fade gradually between on and off. This simulates the effect of the third velocity component of the physical flow that conveys particles across the light sheet. Though particle appearance/disappearance and noise are not related in real world, sequences mixed with the "Noise $N$%" and "Add/rm $N$%" effects added are generated and labelled "Mixed $N$%" simply to set reference points with both perturbations.

For all sequences the interior of the circles that represent the cylinders around which the particles flow are filled with a fixed texture distinct from the particle texture. The motion at these boundaries and inside the cylinders must be zero. The velocity field leads to a mean displacement module of 7.58 pixels/frame and a maximum displacement of 13.5 pixels/frame. Figure 5 (top) shows one image of a synthetic

| | DPIV32 | DPIV48 | ODP2 | ODP4S | ODP4M |
|---|---|---|---|---|---|
| Perfect | 0.55±0.94 | 0.87±1.46 | 0.13±0.10 | 0.13±0.54 | 0.07±0.07 |
| Noise 5% | 0.61±1.18 | 0.86±1.49 | 0.21±0.46 | 0.10±0.13 | 0.08±0.08 |
| Noise 10% | 0.77±1.57 | 0.91±1.59 | 0.53±1.44 | 0.17±0.53 | 0.11±0.09 |
| Noise 20% | 3.11±4.14 | 2.06±2.88 | 0.88±1.58 | 0.30±0.68 | 0.20±0.14 |
| Add/rm 5% | 0.55±0.90 | 0.86±1.45 | 0.14±0.11 | 0.08±0.11 | 0.07±0.08 |
| Add/rm 10% | 0.55±0.93 | 0.87±1.47 | 0.34±1.28 | 0.14±0.56 | 0.08±0.09 |
| Add/rm 20% | 0.56±0.99 | 0.88±1.52 | 0.16±0.12 | 0.18±0.69 | 0.10±0.10 |
| Mixed 5% | 0.60±1.12 | 0.86±1.51 | 0.20±0.13 | 0.15±0.53 | 0.09±0.08 |
| Mixed 10% | 0.91±1.89 | 0.93±1.66 | 0.57±1.71 | 0.20±0.59 | 0.13±0.11 |
| Mixed 20% | 3.73±4.39 | 2.49±3.19 | 0.74±0.52 | 0.43±1.08 | 0.27±0.22 |

**Table 1**
Absolute velocity error in pixels/frame (relative to a mean velocity module of 7.58 pixels/frame)

sequence and the original velocity field used to generate the synthetic sequences. For clarity, in the figure, the velocity vectors are subsampled 16 times in both directions and are displayed using a non linear scale which emphasizes small vectors relative to large ones (the direction of the vector is conserved but its length is proportional to the square root of the velocity module instead of to the module itself). This allows to visualize the flow structure simultaneously in high and low speed regions.

The sequences of synthetic images were evaluated using the classical 2D DFT based DPIV method and the new ODP-PIV algorithm. For the cross-correlation DPIV, two search window sizes were applied: 32×32 (DPIV32) and 48×48 (DPIV48). For the ODP-PIV evaluation, three variants were investigated. The first one (ODP2) uses only 2 images (indices 1 and 2) like in the classical DPIV. The second (ODP4S) and third (ODP4M) variant use 4 images (indices 0, 1, 2 and 3); they differ in the generalized pixel to pixel distance definition: the ODP4S variant uses definition (1) whereas the ODP4M variant uses definition (2):

$$d(p_0, p_1, p_2, p_3) = \sum_{i=0}^{i=2} \mid p_{i+1} - p_i \mid \qquad (1)$$

$$d(p_0, p_1, p_2, p_3) = (\max_{i=0}^{i=3} p_i) - (\min_{i=0}^{i=3} p_i) \qquad (2)$$

For each evaluated case, the velocity error is computed for the whole image (neither holes nor border offset), except at the inner surface of the circles the particles are moving around. Table 1 displays the absolute velocity error which is given as the $L_1$ norm of the difference between the correct and computed velocity in pixels/frame. Figure 5 (bottom) shows the velocity fields obtained using ODP-PIV (for the mixed 20% test), using two or four images.

For the classical DPIV method, the vector set is sparse (about 0.3% density), whereas it is dense (100% density) for the ODP-PIV method. The DPIV method appears to be rather insensitive to particle appearance/disappearance, but on the other hand, it is very sensitive to the introduced noise. As one would expect for the classical DPIV method, expanding the search window size increases its robustness to noise but, simultaneously, decreases the accuracy. The ODP-PIV method appears equally sensitive to both introduced disturbances, but its performance is far better than that of the classical DPIV method in all investigated cases.

## 5 Results on real particle images

The ODP-PIV method was applied to a four image sequence taken from an experiment of water freezing in a lid cooled cubical cavity [14]. The objective of the experiment was to check the validity of corresponding numerical

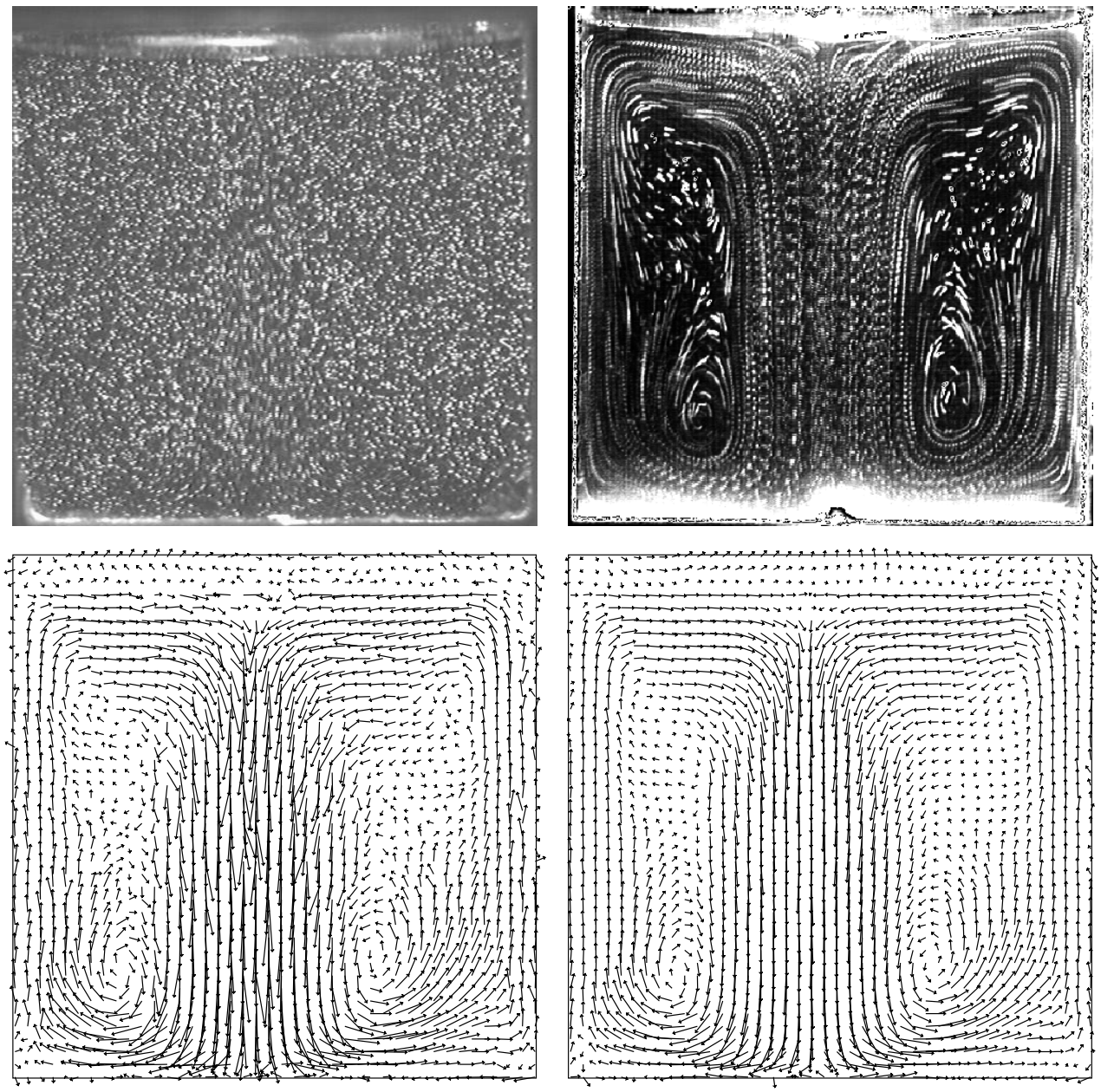

**Fig. 6.** Real particle sequence (four 496 × 496 images). Water freezing in a lid cooled cubical cavity. Top left: particle image; top right: 15 superimposed similar images; bottom left and right: recovered velocity fields from two images and four images. Velocity fields are displayed using a non linear scale. The average module of the extracted velocity field is of 4.4 pixels/frame with a maximum of 27.4 pixels/frame.

simulations of the thermally driven internal flows [18]. A conical ice crystal develops at the cavity top wall. The four images are taken every 200ms, at 308s after the temperature difference is set. Figure 6 shows one of the image of the sequence, fifteen similar images superimposed and the velocity fields obtained from the ODP-PIV method using the ODP2, and the ODP4S variants. The average module of the extracted velocity field is about 4.4 pixels/frame with a maximum as high as 27.4 pixels/frame. According to our calibration, we

estimate that the average accuracy is below 0.5 pixel/frame for the ODP2 variant and below 0.2 pixel/frame for the ODP4M and ODP4S variants.

For $N \times N$ images, the asymptotic computation time is $O(N^3 \log N)$ for all the ODP variants but there is a portion of the algorithm with a $O(N^2 \log N)$ computation time that still has a significant impact for $N$ values within a few hundreds. Practically, doubling the image size $N$ increases the computation time by roughly six times. It is possible to turn off some quality options and significantly reduce (by up to three times) the computation time at the price of a loss in accuracy. With all options tuned towards the highest quality, using a 333 Mhz Pentium II processor with Linux OS, for 496 × 496 images, the ODP2, ODP4S and ODP4M variants take about 10, 102 and 95 minutes respectively. The ODP2 variant itself can be seen as a lower quality / faster speed option for ODP4 variants. Using shrinked (248 × 248) images, the ODP2 variant takes about 1.5 minute and less than 0.5 minute with all options tuned towards the fastest speed, and still produces a usable flow field (not shown).

## 6 Results on smoke images

The ODP-PIV method was also successfully applied to smoke and sand image sequences. Though no tracer particle is individually visible in these images, there is is still a local texture (variation of smoke or sand density) that is carried by the flow field. The ODP-PIV is able to accurately track this texture and recover the flow field. Currently, no known classical DPIV method is able to extract any usable flow field from this type of sequences.

The original image sequence was taken on a video tape by Y.Levy from Technion, Israel using a high speed acquisition system (100 Hz image rate / 200 Hz field rate). A sand burst is created and then it collapses. The air motion around is visualized by smoke injection. The images were digitized at IPPT-PAN for evaluation. The useful area is 700 × 416 pixels.

There were two difficulties with the digitized data. First difficulty was that the digitized images were interlaced with significant motion from field to field. Then, all images were split into fields and complete images were rebuilt by interpolating the missing lines in order to keep the same aspect ratio and image alignment. This leads to a sequence with a number of images and an image rate double of that of the original sequence.

Second difficulty was that the images in the digitized data were not consecutive (one of every two images was digitized in the interesting portion of the sequence). Therefore, the spacing between consecutive field images is not constant (5 ms for fields from the same original image and 15 ms for fields from subsequent images). This is not a problem for the ODP2 variant that takes only two images but the ODP4 variants that uses four or more images require them to be equally spaced. The problem was overcome by synthesizing the two intermediate missing field images using the nearest field images and the velocity field obtained from them using the ODP2 variant [10]. Then, the ODP4M variant was run with six (two original, two synthesized and two original) field images. In fact, the impact of the intermediate field images is small since they have a small motion amplitude and the flow field is obtained from nothing else but the four original fields (and, actually, from two original two-field images).

Figure 7 shows the results for two pairs of two-field images. It shows original field images, velocity fields obtained using two and four original field images. Results are better with four field images but a usable velocity field is already obtained with only two field images. The figure also shows enlarged portions of the extracted velocity fields showing the high resolution of the method. The sand motion was also well recovered using the ODP-PIV.

## 7 Results on bubble images

In order to investigate the possible use of ODP-PIV for other fluid mechanics experiment analy-

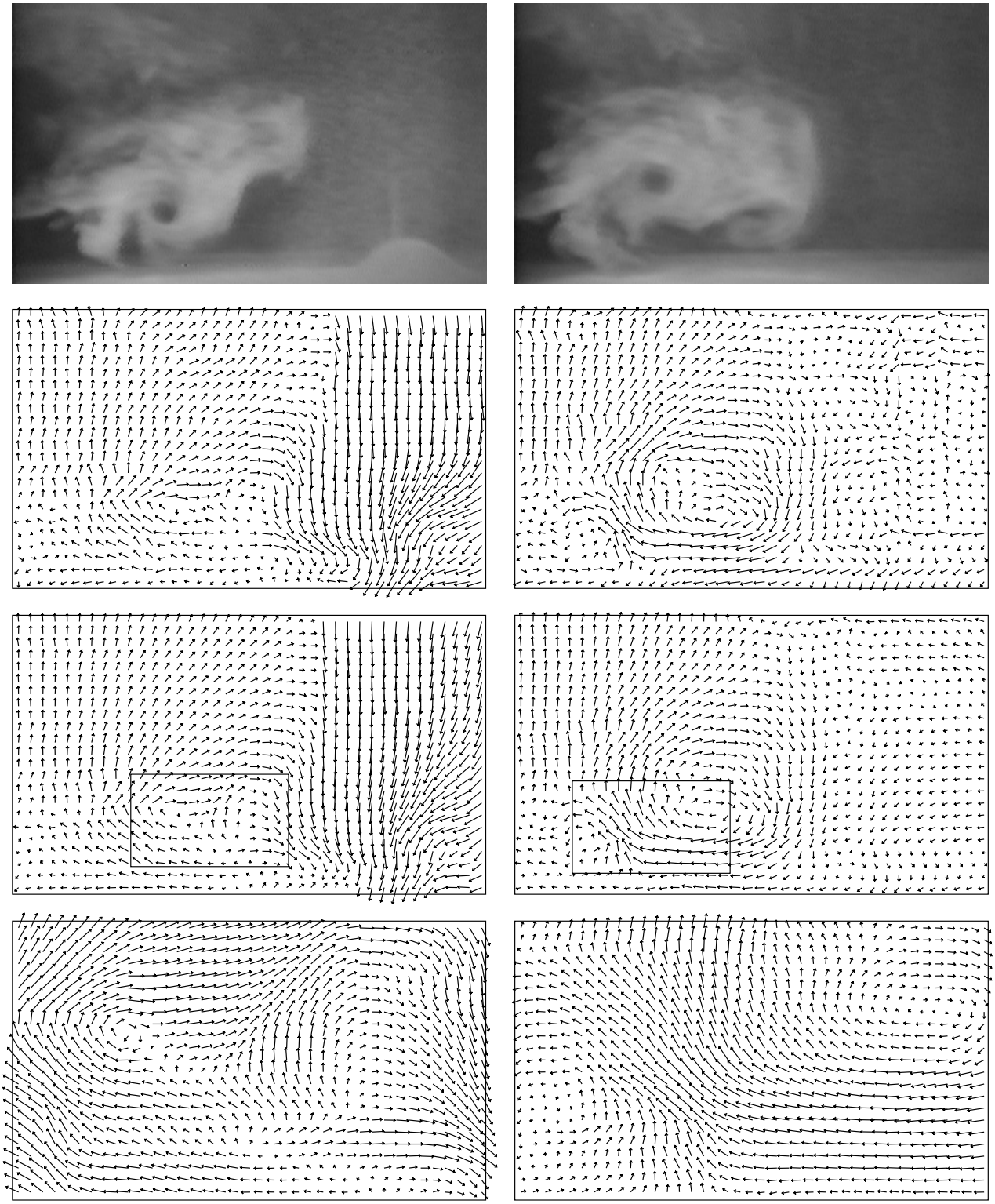

**Fig. 7.** Smoke sequences (four 700 × 416 images, extracted from a longer sequence taken by Y. Levy, Technion, Israel). Top row: images from the original sequence; middle top row: velocity fields from 2 images (subsampled 18 times horizontally and vertically); middle bottom row: velocity fields from 4 images (subsampled 18 times); bottom row: 3x zoom of a portion of the velocity fields (subsampled 6 times). Velocity fields are displayed using a non linear scale.

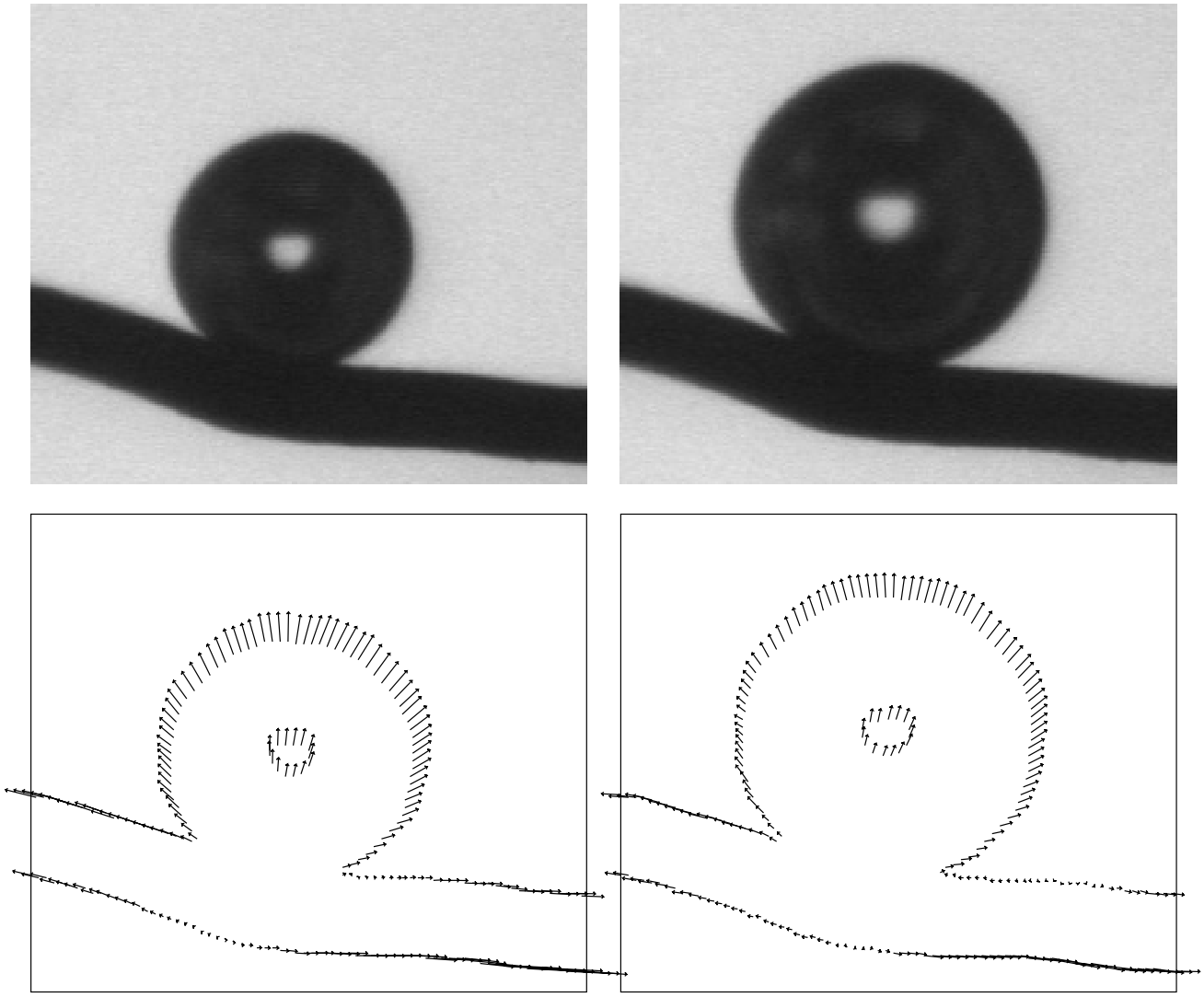

**Fig. 8.** Bubble sequence (nine 215 × 185 images). Microsopic images of a vapor bubble growing on a thin heated wire. Methyl alcohol, images taken every 40ms, illumination time 100ns, mean bubble diameter 180um. Top left and right: first and last image of the sequence, bottom left and right: velocities obtained from the first four and the last four images of the sequence. Velocity fields are computed on the whole image but displayed only on contours. Vectors represent the displacement between the first and last image used fot the computation (absolute scale).

sis, it was tried on an image sequence of a vapor bubble growing on a thin heated wire [7]. The is no clearly visible texture in the fluid or bubble but the ODP-PIV successfully recovered a velocity field on the bubble contour. The velocity field was computed on the whole image and looked consistent with the data but it is expected to be reliable only on textured area, here essentially on bubble contour, and only for the component orthogonal to the contour. Figure 8 shows images from the sequence and the velocities extracted on contour points.

## 8 Conclusion

An Optical Flow technique based on the use of Dynamic Programming has been successfully applied to Particle Image Velocimetry yielding a significant increase in the accuracy and spa-

tial resolution of the velocity field. Results have been presented for calibrated synthetic sequences and for real sequences from an experiment on natural convection in freezing water. Using the ODP-PIV, a dense velocity vector field for every pixel of the image is obtained. For calibrated particle images, accuracy is better than 0.5 pixel/frame for two-image sequences and better than 0.2 pixel/frame for four-image sequences, even with a 10% noise level and a 10% rate of appearance and disappearance of particles. The ODP method has also been successfully applied on smoke and bubble image sequences on which all other classical DPIV methods fails.

## Acknowledgements

We acknowledge support from the Conjoint CNRS-PAN Project No. 2930. The third author acknowledges support of the State Scientific Committee (KBN Grant No. 3P40400107).

## References

[1] Barron J. L, Fleet D. J, and Beauchemin S. S. Performance of optical flow techniques. *International Journal of Computer Vision*, Vol. 12, pp 43–77, 1994.

[2] Hesselink L. Digital image processing in flow visualization. *Ann. Rev. Fluid Mech.*, Vol. 20, pp 421–485, 1988.

[3] Huang H. T, Fiedler H. E, and Wang J. J. Limitation and improvement of piv. part i: Limitation of conventional techniques due to deformation of particle image patterns. *Exp Fluids*, Vol. 15, pp 168–174, 1993.

[4] Lourenco L and Krothapalii A. On the accuracy of velocity and vorticity measurements with piv. *Exp Fluids*, Vol. 19, pp 421–428, 1995.

[5] Lu H. Z. Simulation des écoulements externes visqueux incompressibles par une méthode de couplage: Différences finies particulaires. Technical report, Notes et documents LIMSI No 96-10, 1996.

[6] Merzkirch W and Gui L. C. A method of tracking ensembles of particle images. *Exp Fluids*, Vol. 21, pp 465–468, 1996.

[7] Pakleza J and Kowalewski T. A. Messures de la vitesse de deplacement de l'interface liquide - vapeur des bulles en ebullition nucleee. *Proc Journees du GREDIC (GDR 1205 CNRS)*, 24-25 February 1998.

[8] Quénot G. M. The "orthogonal algorithm" for optical flow detection using dynamic programming. *Proc International Conference on Acoustics, Speech and Signal Processing*, Vol. 3, pp 249–52. IEEE New York, NY, USA, 23-26 March 1992.

[9] Quénot G. M. Computation of optical flow using dynamic programming. *Proc Intl. Workshop on Machine Vision Applications*, pp 249–52, 12-14 November 1996.

[10] Quénot G. M. Image matching using dynamic programming: Application to stereovision and image interpolation. *Proc IMAGE'COM*, pp 265–70, 20-22 May 1996.

[11] Quénot G. M, Pakleza J, and Kowalewski T. A. Particle image velocimetry with optical flow. *Experiments in fluids*, Vol. 25, No 3, pp 177–189, August.

[12] Sakoe H and Chiba S. Dynamic programming optimization for spoken word recognition. *IEEE Trans. Acoust., Speech, and Signal Proc.*, Vol. 26, pp 43, 1978.

[13] Sun J. H, Yates D. A, and Winterbone D. E. Measurement of the flow field in a diesel engine combustion chamber after combustion by cross-correlation of high-speed photographs. *Exp Fluids*, Vol. 20, pp 335–345, 1996.

[14] T. A. Kowalewski A. C. Natural convection with phase change (in polish). Technical report, IPPT PAN Reports 4/1997, 1997.

[15] Tokumaru P. T and Dimotakis P. E. Image correlation velocimetry. *Exp Fluids*, Vol. 19, pp 1–15, 1995.

[16] Westerweel J. *Digital Particle Image Velocimetry - Theory and Application.* Delft University Press, 1993.

[17] Willert C. E and Gharib M. Digital particle image velocimetry. *Exp Fluids*, Vol. 10, pp 181–193, 1991.

[18] Yeoh G. H. *Natural convection in a solidifying liquid.* Ph.d. thesis, University of New South Wales, Kensington, Australia, 1993.